engineering proceedings

MDPI

Proceeding Paper

Self-Healing Thermosetting Load-Bearing Resins: Morphological and Mechanical Properties †

Marialuigia Raimondo [1,*], Elisa Calabrese [1], Luigi Vertuccio [2] and Liberata Guadagno [1]

[1] Department of Industrial Engineering, University of Salerno, 84084 Fisciano, Italy; elicalabrese@unisa.it (E.C.); lguadagno@unisa.it (L.G.)
[2] Department of Engineering, University of Campania "Luigi Vanvitelli", 81031 Aversa, Italy; luigi.vertuccio@unicampania.it
* Correspondence: mraimondo@unisa.it
† Presented at the 15th EASN International Conference, Madrid, Spain, 14–17 October 2025.

Abstract

This paper focuses on developing reinforced self-healing supramolecular resins that meet both functional and structural needs for industrial use. The formulated advanced nanocomposites are made from compounds that allow for reversible self-healing interactions. The self-healing molecules bond with the toughened epoxy matrix using hydrogen bonding. To enhance the epoxy's typical insulating properties, electrically conductive carbon nanotubes (CNTs) were added to achieve an electrical percolation threshold (EPT) with a low amount of nanofiller. This study found that self-healing efficiency can reach nearly 99%. The addition of healing compounds significantly raises the glass transition temperature to over 200 °C. Tunneling Atomic Force Microscopy (TUNA), which is an innovative tool for correlating local topography with electrical properties, reveals the structural properties and compatibility of these materials, mapping conductive pathways at the micro- and nanoscale.

Keywords: tunneling atomic force microscopy (TUNA); mechanical properties; thermosetting resins; carbon nanotubes; molecular self-healing fillers; smart materials; reversible interactions

1. Introduction

This research investigates multifunctional self-healing supramolecular toughened resins designed to mitigate the insulating characteristics of epoxy polymers while incorporating auto-repair mechanisms. These nanocomposites, formed from materials that enable reversible self-healing mechanisms, are characterized morphologically and mechanically through Tunneling Atomic Force Microscopy (TUNA) and Fracture Tests, respectively. The selected self-healing molecules are capable of forming non-covalent interactions with the hydroxyl (OH) and carbonyl (C=O) groups present in the reinforced epoxy matrix, utilizing their hydrogen-bonding donor and acceptor properties [1,2]. Moreover, they can work well with the polymer matrices employed for hosting and can establish strong, reversible, and attractive interactions. They efficiently generate combined outcomes resulting from reversible interactions driven by hydrogen bonding within the epoxy matrix [3–5]. TUNA highlights key structural characteristics of CNTs, their dispersion within the polymer matrix, and their compatibility with the globular rubber domains.

The TUNA method charts the electrical conductivity of samples in micro- and nanoscale spatial regions [6]. Identifying electrical currents uncovers supra-molecular

Check for updates

Academic Editors: Spiros Pantelakis, Andreas Strohmayer and Gustavo Alonso

Published: 18 May 2026

Copyright: © 2026 by the authors. Licensee MDPI, Basel, Switzerland. This article is an open access article distributed under the terms and conditions of the Creative Commons Attribution (CC BY) license.

networks, dictated by hydrogen bonds, in the samples, highlighting the morphological characteristics of the sample with an embedded conductive nano-filler in the hosting matrix.

In particular, the concurrent collection of various TUNA images, including Height, Deflection Error, Friction, and TUNA Current, offers a thorough insight into the morphological and electrical characteristics of the sample [7,8], thus allowing the precise identification of the locations of conductive paths and interconnections within the epoxy matrix, even at low concentrations of conductive fillers.

The self-healing (*SH*) performance, evaluated through fracture testing, can attain nearly full self-repair capability (SH = 98.9%) depending on the precise chemical composition. Incorporating healing compounds bonded to the epoxy matrix leads to a significant rise in Tg, with values exceeding 200 °C. Furthermore, high storage modulus values ranging from 5000 to 2000 MPa up to 60 °C have been recorded. Epoxy composites filled with CNTs and self-healing fillers proved to be a winning combination. This strategic approach appears to serve as a sound basis for integrating self-reactive functions dependent on the material's electrical characteristics, including self-sensing, de-icing, and/or anti-icing derived from the Joule effect of current flowing through the composite material. The characterizations performed demonstrate that this particular combination can offer effective solutions for producing "smart" and "multifunctional" resins with a high Tg, using commercially accessible materials and avoiding synthesis processes, thus minimizing the time and expenses related to composite formulation.

2. Materials and Methods

The smart materials consist of an epoxy matrix filled with CNTs and self-repairing fillers. The preparation of every sample involved using an epoxy-to-block copolymer (E/B) at a ratio of 80/20. In the samples containing the elastomeric phase denoted as C, this component was incorporated at a concentration of 12.5 parts per hundred resin (phr) relative to the epoxy precursor (E). It was chemically bonded to the epoxy matrix through a covalent reaction facilitated by triphenylphosphine (PPh_3), which was employed at a concentration of 10 phr based on E. Additionally, the curing agent H was introduced at a concentration of 55 phr with respect to E, while the carbon nanotubes and self-healing fillers were introduced at 0.5 wt% and 1.0 wt%, respectively, with respect to the Ep epoxy sample, which has the composition E + B + C + H. In particular, the selected CNTs percentage was based on the criterion of optimizing electrical properties [1]. The incorporation of self-healing fillers leads to a dual impact: a reduction in curing temperature and a concomitant decrease in the degree of curing achieved.

The chosen self-healing filler percentage was made to obtain a good self-healing performance, together with a curing degree exceeding 90%. This enables the materials to be appropriate for use in structural applications [1].

Figure 1a provides details on the individual components, and Figure 1b presents a schematic depiction of the chemical structures of the healing molecules, highlighting the hydrogen bonding interactions they form. These interactions occur between the carbonyl groups, which serve as hydrogen-bond acceptor sites, and the hydroxyl groups, which act as hydrogen-bond donor sites within the reinforced matrix. The diagram demonstrates the reversible interactions that depend on hydrogen bonds, shown by dashed lines.

Figure 2 presents details regarding the samples examined in this study.

The minimal inclusion of carbon nanofillers renders the samples electrically conductive, enabling them to achieve the electrical percolation threshold (EPT). They underwent a two-phase curing procedure: first at a minimum temperature of 125 °C for 1 h and subsequently at a maximum temperature of 200 °C for 3 h.

https://doi.org/10.3390/engproc2026133153

Compound	Description	Acronym
Tetra glycidyl methylene dianiline *	Tetrafunctional epoxy precursor, viscous liquid	E
1,4-butanedioldiglycidylether *	Reactive diluent, liquid	B
Carboxyl terminated butadiene acrylonitrile **	Toughening Elastomer, viscous liquid	C
4,4′-diaminodiphenyl sulfone *	Hardening agent, powder	H
Multiwall carbon nanotubes ***	Conductive filler (3100 Grade), powder	CNT
1,3-Dimethylbarbituric acid *	Self-healing filler, powder	D
2-Thiohydantoin *	Self-healing filler, powder	T
Murexide *	Self-healing filler, powder	M

* Purchased by Merck (Merck KGaA Darmstadt, Germany). ** Supplied by Hycar-Reactive Liquid Polymers (Huntsman Corporation, 10003 Woodloch Forest Dr, The Woodlands, TX 77380, USA). *** Purchased by Nanocyl S.A. (Sambreville, Belgium).

(**a**)

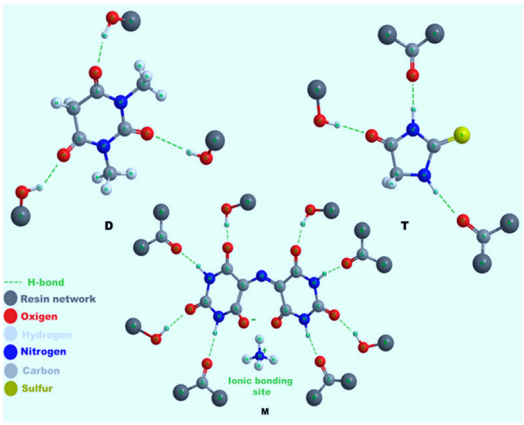

(**b**)

Figure 1. Information about the separate compounds (**a**), diagrammatic depiction of the chemical structures of the healing agents and the hydrogen bonding interactions (**b**).

Sample Composition	Description	Acronym
E + B	Uncured viscous liquid sample	EB
E + B + C	Uncured viscous liquid sample	EBC
E + B + self-healing filler	Uncured viscous liquid sample	EB-D
		EB-T
		EB-M
E + B + C + self-healing filler	Uncured viscous liquid sample	EBC-D
		EBC-T
		EBC-M
E + B + C + H	Oven-cured epoxy sample	Ep
E + B + C + H + CNT	Oven-cured epoxy sample	Ep-CNT
E + B + C + H + self-healing filler	Oven-cured epoxy sample	Ep-D
		Ep-T
		Ep-M
E + diluent + C + H + CNT + self-healing filler	Oven-cured epoxy sample	Ep-CNT-D
		Ep-CNT-T
		Ep-CNT-M

Oven-cured: two-stage curing cycle, namely 1 h at 125 °C and 3 h at 200 °C.

Figure 2. Details regarding the samples examined in this study.

The TUNA images were analyzed using the Bruker software Nanoscope Analysis 1.80 (Build R1.126200). Ref. [6] offers information regarding the acquisition parameters. The sample slices were etched before the TUNA observation.

The self-healing capability (*SH*) of all epoxy-cured samples was assessed, as outlined in Equation 1, through Tapered Double Cantilever Beam (TDCB) fracture tests (INSTRON mod. 5967 Dynamometer (Inston, Norwood, MA, USA) featuring a 30 KN load cell and a displacement speed of 0.25 mm/min).

$$SH = \frac{P_H}{P_0} \times 100 \quad (1)$$

In the dynamic mechanical analysis (DMA), solid samples shaped as cuboids ($2 \times 10 \times 35$ mm^3) were subjected to variable flexural deformation in a three-point bending configuration (Tritec 2000 DMA, Triton Technology Ltd., Worcester, MA, USA) at a

frequency of 1 Hz, with a displacement amplitude of 0.03 mm, and temperatures ranging from −90 °C to 315 °C at a rate of 3 °C min^{-1}.

3. Results and Discussion

Figure 3 illustrates the morphological depiction of the etched epoxy samples Ep-CNT, Ep-CNT-D, Ep-CNT-T, and Ep-CNT-M.

Morphological evaluations were performed to examine the distribution of conductive nanoparticles and self-healing molecules in the rubber-modified toughened polymer matrix.

It is important to highlight that the etching procedure partially takes away the outer layers of the epoxy matrix. Reversible self-healing interactions were analyzed, leveraging the molecular structures equipped with functional groups capable of establishing hydrogen bonds both within the epoxy matrix and between themselves. To prevent any movement of the rubbery phase chains, the surfaces of the samples were prepared by fracturing them under liquid nitrogen conditions. Examination of the FESEM image for the Ep-CNT sample reveals distinct globular domains belonging to the rubber phase. These domains are uniformly distributed and exhibit consistent diameters throughout the solid continuous phase, underscoring their effective integration. The oxidizing action of the etching solution further enhanced the visibility of these globular domains by selectively eroding the interface between the rubber phase and the epoxy matrix, which is characterized by a lower cross-link density. The TUNA analysis confirmed a homogeneous dispersion of nanofillers in all three samplesEp-CNT-D, Ep-CNT-T, and Ep-CNT-M. This uniform distribution enabled the formation of a continuous conductive network securely anchored to the epoxy matrix through reversible, non-covalent bonds. TUNA current imaging provided nanoscale electric current readings, showing a range from −351.2 fA to 339.9 fA for the Ep-CNT-D sample, from −321.1 fA to 324.2 fA for Ep-CNT-T, and from −2.3 pA to 5.0 pA for Ep-CNT-M.

The electrical conductivity values determined for the multifunctional self-healing systems Ep-CNT-D, Ep-CNT-T, and Ep-CNT-M were 1.15×10^{-2} S/m, 2.27×10^{-4} S/m, and 1.29×10^{-2} S/m, respectively. For the sample Ep-CNT, which demonstrated an electrical conductivity of 2.56×10^{-2} S/m, the recorded electric current ranged between −506.4 fA and 484.9 fA. These findings highlight that the observed current flow, driven by the tunnel effect of the conductive nanofiller, facilitates effective transmission of electrical properties to the insulating matrix Ep, which itself exhibits a notably low electrical conductivity of 1.16×10^{-14} S/m.

Unmodified carbon nanotubes, together with self-healing additives, exhibit excellent dispersion in the resin.

Figure 4 presents a histogram illustrating the critical fracture load values for both the virgin (P_0) and healed (P_H) cured nanocomposites, specifically Ep-CNT, Ep-CNT-D, Ep-CNT-T, and Ep-CNT-M.

The favorable healing efficiency values (exceeding 65% for all samples) lead us to assume a synergistic effect among the different components (CNT and self-healing filler), which, by interacting within the mixture, might form a supramolecular network capable of initiating self-healing processes. In this context, it is important to highlight that the epoxy matrix naturally has a limited capacity for self-repair because of the numerous -OH groups created during the cross-linking process, which contribute to the structure's hardened state. Cured epoxy resins (hardened with primary aromatic amines, such as DDS) can also undergo reversible hydrogen bonding from the -OH groups. In comparison, for the reference sample Ep-CNT, the mere presence of CNTs leads to a 15% enhancement in healing efficiency in the absence of self-healing fillers. Consequently, the co-existence of CNTs along with self-healing fillers (D, T, and M) led to an enhancement in the self-healing ability of the nanocomposites. In reality, elevated S_H values were noted, specifically

81.1% for Ep-CNT-D, 65.5% for Ep-CNT-T, and 98.9% for Ep-CNT-M. The self-healing efficiency of the nanocomposites is closely linked to the chemical structure of the self-healing fillers, specifically to the type and amount of functional groups in the molecule that can engage in hydrogen bonding. The sample containing filler M showed the greatest S_H value, featuring more hydrogen-bonding donor and acceptor sites compared to the other two compounds, D and T.

The Ep-CNT-M composite fully restores the damage, and the maximum efficiency value achieved for this sample may be a result of the molecule's chemical properties. The M filler has more sites for hydrogen bonding donation and acceptance compared to the other two compounds. Moreover, it showcases locations that can form ionic interactions.

Figure 5 presents the DMA results of the examined samples: (a) Tan δ curves as a function of temperature; (b) temperatures at which Tan δ reaches its maximum; (c) storage modulus as a function of temperature; (d) storage modulus values at varying temperatures (−25, 30, and 150 °C).

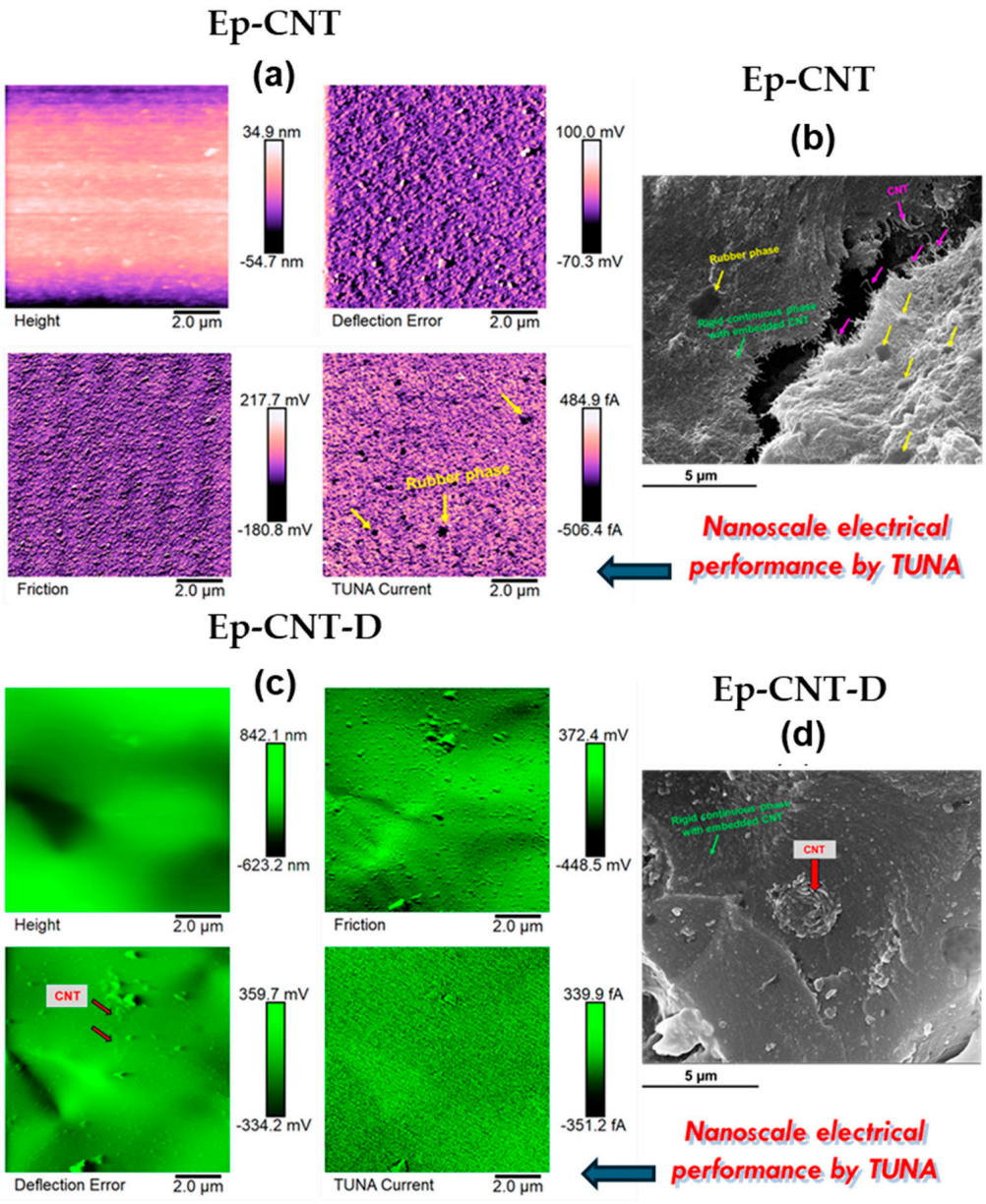

Figure 3. *Cont.*

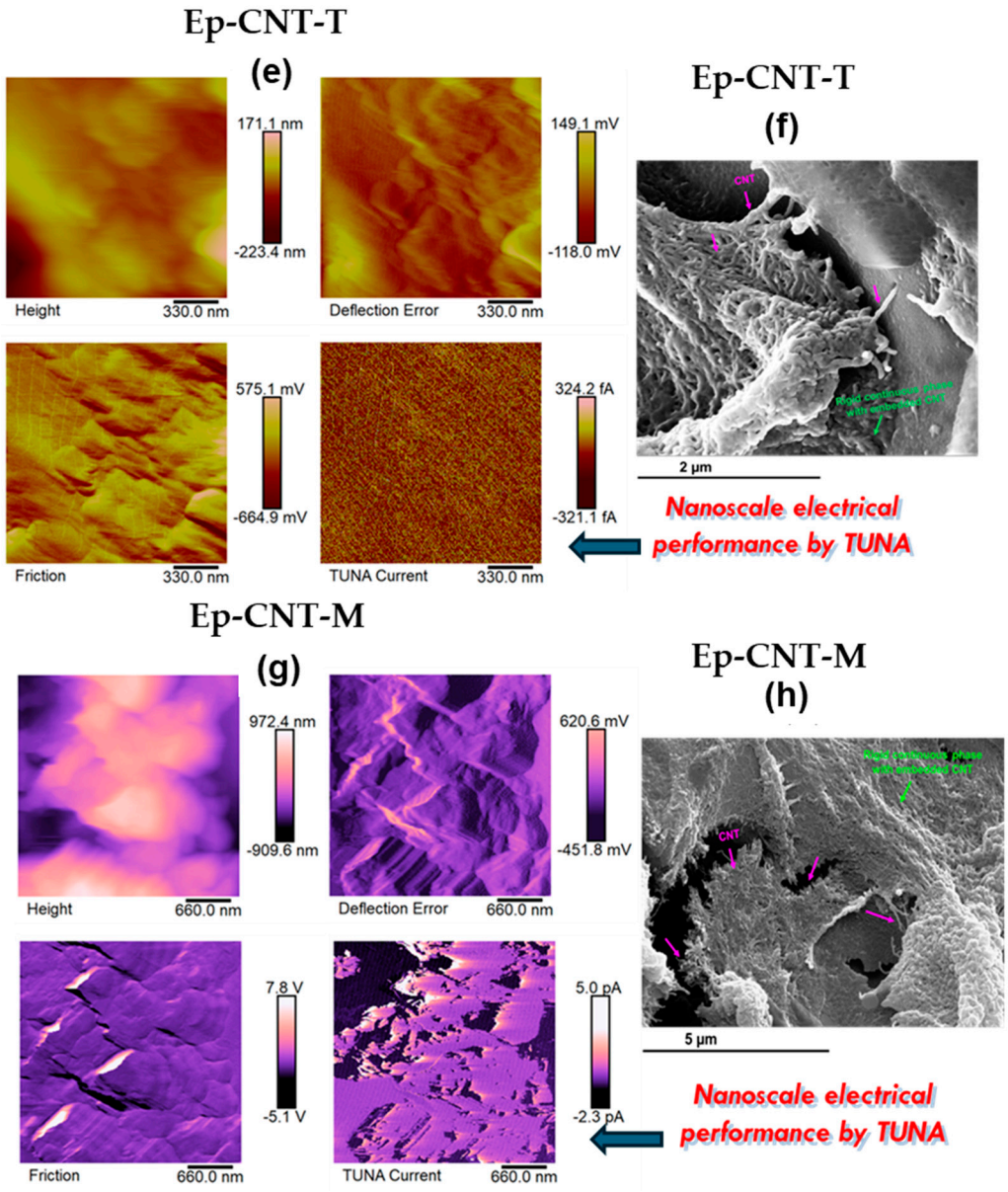

Figure 3. Morphological representation of epoxy samples. Ep-CNT: (**a**) TUNA images; (**b**) FESEM image. Ep-CNT-D: (**c**) TUNA images; (**d**) FESEM image. Ep-CNT-T: (**e**) TUNA images; (**f**) FESEM image. Ep-CNT-M: (**g**) TUNA images; (**h**) FESEM image. Yellow arrows indicate the rubber phase, fuchsia arrows indicate the CNT, and green arrows indicate the rigid continuous phase with embedded CNT.

Dynamic Mechanical Analysis (DMA) was employed to assess the influence of CNT and D, T, and M components added to impart self-healing capability to the resin and to study the glass transition temperature (Tg) and storage modulus of the cured samples. The results of these tests are illustrated in Figure 5. Examination of the curves in Figure 5a reveals that, except for the sample containing filler D, the incorporation of carbon nanotubes (CNTs) together with the self-healing fillers into the Ep matrix leads to a noticeable increase in Tg, rising from 190 °C to 216 °C (Figure 5b). Furthermore, an increase in storage modulus within the low-temperature range (−90 °C to 0 °C) is observed for the sample containing only CNTs (black curve in Figure 5c). At temperatures above 0 °C, the difference between Ep and Ep-CNT becomes negligible (Figure 5d). Interestingly, when CNTs are combined with self-healing fillers, the storage modulus decreases across the entire temperature range, followed by a sharp decline starting near 150 °C.

https://doi.org/10.3390/engproc2026133153

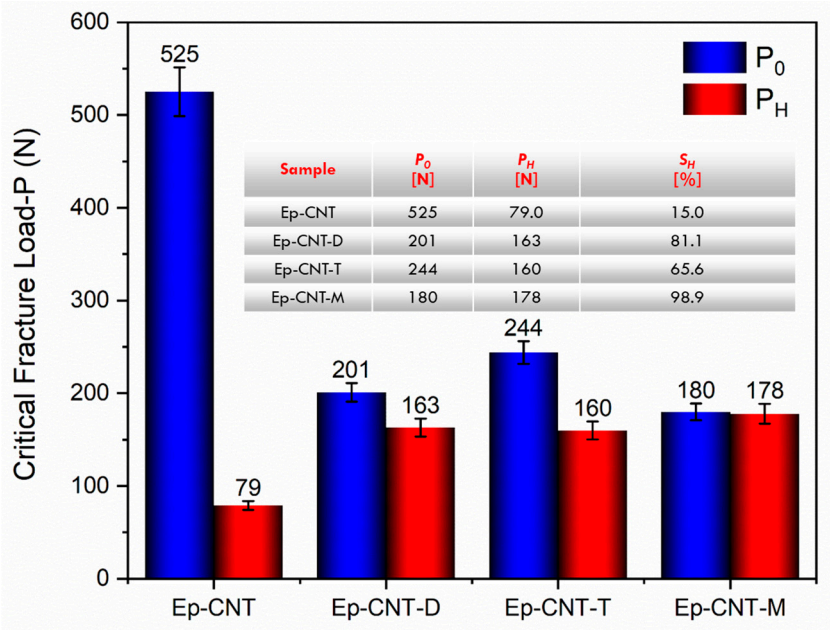

Figure 4. Histogram of the critical fracture load values for the virgin (P_0) and the healed (P_H) epoxy nanocomposites.

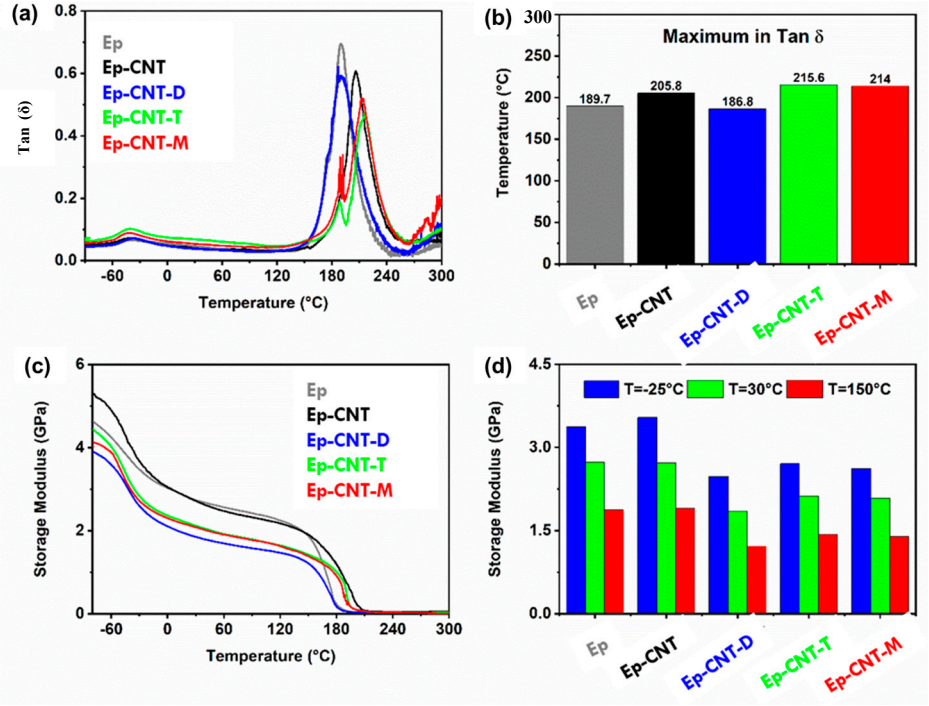

Figure 5. DMA results of the examined samples: (**a**) Tan δ curves as a function of temperature; (**b**) temperatures at which Tan δ reaches its maximum; (**c**) storage modulus as a function of temperature; (**d**) storage modulus values at varying temperatures (−25, 30, and 150 °C).

4. Conclusions

In this study, we performed an in-depth analysis of multifunctional self-healing supramolecular systems, focusing on both morphological and mechanical aspects. Morphological characterization was carried out using Tunneling Atomic Force Microscopy (TUNA), which enabled nanoscale mapping of conductive pathways, while fracture tests assessed the mechanical integrity and damage recovery capability of the materials. The incorporation of self-healing fillers significantly improved thermal stability, increasing the glass

transition temperature (Tg) to values exceeding 200 °C without disrupting the continuity of the conductive network. This was confirmed by favorable nanoscale electrical current measurements, which, together with the positive results from self-healing efficiency evaluations, validate the proposed design strategy for developing multifunctional, load-bearing materials with autonomous repair capability. The healing mechanism relies on reversible supramolecular interactions, primarily hydrogen bonding and π–π stacking between functional groups within the matrix and the self-healing moieties. Upon mechanical damage, these dynamic bonds dissociate and subsequently reform when the material is exposed to mild thermal activation or environmental stimuli, enabling efficient crack closure and restoration of structural integrity. This process occurs without external intervention or additional chemicals, ensuring repeatable healing cycles and preserving the material's conductive and mechanical properties over time. Such advanced materials present significant opportunities for high-performance applications where durability, reliability, and multifunctionality are critical. Potential uses include aerospace and automotive components, where high thermal resistance and mechanical strength are essential; electronic devices and flexible circuits, which benefit from maintained conductivity and autonomous repair under operational stress; and renewable energy systems, such as wind turbine blades or solar panel supports, where extended service life and reduced maintenance costs are highly desirable. Furthermore, these supramolecular systems could be integrated into smart infrastructure and wearable technologies, enabling safer, longer-lasting, and more sustainable solutions across multiple sectors.

Author Contributions: Conceptualization, L.G. and M.R.; methodology, L.G., E.C. and M.R.; software, L.V. and E.C.; validation, L.G. and M.R.; formal analysis, E.C., L.V. and M.R.; investigation, E.C., L.V. and M.R.; resources, L.G.; data curation, L.G., L.V. and E.C.; writing—original draft preparation, M.R.; writing—review and editing, M.R.; visualization, E.C., L.V. and L.G.; supervision, L.G. and M.R.; project administration, L.G. and M.R. All authors have read and agreed to the published version of the manuscript.

Funding: The authors gratefully acknowledge the PRIN 2022 project "Integration of Continuous Fibers and Self-healing agents in 3D printed thermoplastic composites (INFINITE)" (Prot. 2022AKTCPH), funded by the Italian Ministry of University and Research, for financial support.

Institutional Review Board Statement: Not applicable.

Informed Consent Statement: Not applicable.

Data Availability Statement: Data sets are contained within the article. Further data and materials requests should be addressed to the corresponding author.

Conflicts of Interest: The authors declare no conflicts of interest.

References

1. Guadagno, L.; Raimondo, M.; Naddeo, C.; Vertuccio, L.; Russo, S.; Iannuzzo, G.; Calabrese, E. Rheological, Thermal and Mechanical Characterization of Toughened Self-Healing Supramolecular Resins, Based on Hydrogen Bonding. *Nanomaterials* **2022**, *12*, 4322. [CrossRef] [PubMed]
2. Guadagno, L.; Calabrese, E.; Longo, R.; Aliberti, F.; Vertuccio, L.; Catauro, M.; Raimondo, M. Morphological and Spectroscopic Characterization of Multifunctional Self-Healing Systems. *Polymers* **2025**, *17*, 1294. [CrossRef] [PubMed]
3. Liu, T.; Zhao, H.; Zhang, D.; Lou, Y.; Huang, L.; Ma, L.; Hao, X.; Dong, L.; Rosei, F.; Lau, W.M. Ultrafast and high-efficient self-healing epoxy coatings with active multiple hydrogen bonds for corrosion protection. *Corros. Sci.* **2021**, *187*, 109485. [CrossRef]
4. Wang, N.; Feng, X.; Pei, J.; Cui, Q.; Li, Y.; Liu, H.; Zhang, X. Biobased Reversible Cross-Linking Enables Self-Healing and Reprocessing of Epoxy Resins. *ACS Sustain. Chem. Eng.* **2022**, *10*, 3604–3613. [CrossRef]
5. Li, J.; Du, X.; Zhang, A.; Wen, J.; Shuai, L.; Li, S.; Zhu, M.; Nie, Y. Hydrogen-bonded polymeric materials with high mechanical properties and high self-healing capacity. *Mater. Chem. Front.* **2024**, *8*, 3828–3858. [CrossRef]

6. Raimondo, M.; Donati, G.; Milano, G.; Guadagno, L. Hybrid composites based on carbon nanotubes and graphene nanosheets outperforming their single-nanofiller counterparts. *FlatChem* **2022**, *36*, 100431. [CrossRef]
7. Gautier, B.; Fares, B.; Prudon, G.; Dupuy, J.C. Imaging by atomic force microscopy of the electrical properties difference of the facets of oxygen-ion-induced ripple topography in silicon. *Appl. Surf. Sci.* **2004**, *231–232*, 136–140. [CrossRef]
8. Paredes, J.I.; Villar-Rodil, S.; Solís-Fernández, P.; Martínez-Alonso, A.; Tascón, J.M.D. Atomic Force and Scanning Tunneling Microscopy Imaging of Graphene Nanosheets Derived from Graphite Oxide. *Langmuir* **2009**, *25*, 5957–5968. [CrossRef] [PubMed]

Disclaimer/Publisher's Note: The statements, opinions and data contained in all publications are solely those of the individual author(s) and contributor(s) and not of MDPI and/or the editor(s). MDPI and/or the editor(s) disclaim responsibility for any injury to people or property resulting from any ideas, methods, instructions or products referred to in the content.